23rd ABCM International Congress of Mechanical Engineering
December 6-11, 2015, Rio de Janeiro, RJ, Brazil

EVALUATION OF A FATIGUE LIFE ESTIMATION METHODOLOGY FOR VARIABLE AMPLITUDE LOADING

Ouronon Marie Rosalie Beugre
Department of Mechanical Engineering, Polytechnic School, University of São Paulo, 2231 - 05508-900
beugrepamela2@yahoo.fr

Fábio Comes de Castro
Department of Mechanical Engineering, Universidade de Brasília, 70910-900 Brasília, DF, Brazil
fabiocastro@unb.br

Edgar Nobuo Mamiya
Department of Mechanical Engineering, Universidade de Brasília, 70910-900 Brasília, DF, Brazil
mamiya@unb.br

Abstract. *This work presents an evaluation of a methodology for fatigue life estimation, with particular attention to variable amplitude loading. The methodology employs the Chaboche's kinematic hardening model to describe the elastoplastic behavior of the material, and the Bannantine-Socie method to estimate crack initiation life. The evaluation was based on available axial-torsional fatigue tests on S45C and 304 steels. For both steels, most life estimates using the Fatemi-Socie parameter with a variable normal stress sensitivity coefficient were within a factor of two bandwidth. The use of the Smith-Watson-Topper parameter provided a similar overall performance, but life estimates for some of the torsion tests were not satisfactory.*

Keywords: *multiaxial fatigue, fatigue life estimation, variable amplitude loading*

1. INTRODUCTION

Fatigue analysis plays a crucial role in the design of components and structures used in the automotive, aerospace and power generation industries, amongst others. In actual service conditions, such components and structures are often subjected to multiaxial stresses and strains due to the combined action of multiple applied loadings and/or due to the presence of notches. Moreover, loadings encountered in real applications often have a non-proportional and variable amplitude nature.

A widely used methodology for fatigue analysis under variable amplitude loading is the so-called strain-life approach (Socie and Marquis, 2000; Dowling, 2007). It is based on a procedure for identifying and counting loading cycles, a parameter for quantifying the fatigue damage caused by each loading cycle and a rule for estimating the total damage caused by the loading history. Considerable progress has been made on the strain-life approach over the past decades both for uniaxial and multiaxial loading conditions (Wetzel, 1977; Fatemi and Shamsei, 2011). However, the most widely used approaches for variable amplitude multiaxial loads (Bannantine and Socie, 1991; Wang and Brown, 1996) have not yet reached the same degree of maturity of the ones employed for uniaxial conditions. According to the discussion carried out on the First International Workshop on Challenges in Multiaxial Fatigue, held in April 2015 in Urbino, Italy, further work involving more realistic variable amplitude loadings is still required for a proper assessment of current methodologies.

The aim of this paper is to evaluate a methodology for multiaxial fatigue life estimation, with particular attention to variable amplitude loading. In this methodology, the stress-strain analysis is carried out with an elasto-plastic model based on Chaboche's kinematic hardening rule, and the fatigue damage is calculated using the critical plane approach proposed by Bannantine and Socie (1991). Available axial-torsional fatigue tests, conducted with constant and variable amplitude loadings, were used to evaluate the methodology.

2. FATIGUE LIFE ESTIMATION METHODOLOGY

2.1 Critical plane-based fatigue models

Experimental observations have shown that the nucleation and early growth of fatigue cracks occur on a critical plane, i.e. a material plane where the fatigue damage caused by the stresses and strains acting on it is most severe. Based on this phenomenological description of the fatigue cracking process, Brown and Miller (1973) introduced the first critical plane approach for multiaxial low-cycle fatigue, which was later developed by Kandil, Brown and Miller

(1982). According to this approach, crack nucleation is governed by cyclic shear strains while normal strains assist in their early growth. Moreover, an expression for fatigue life estimation was derived as follows:

$$(\Delta\gamma_{\mathrm{max}}{}^{\alpha} + S\Delta\varepsilon_{\mathrm{n}}{}^{\alpha})^{\frac{1}{\alpha}} = f(N_f) \tag{1}$$

where $\Delta\gamma_{\mathrm{max}}$ is the maximum shear strain range, $\Delta\varepsilon_{\mathrm{n}}$ is the normal strain range on the plane of maximum shear strain range, S and α are material constants, and the right-hand side of Eq. (1) is a function of the number of cycles to failure, N_f. Taking as a starting point the approach developed by Brown and Miller, Fatemi and Socie (1988) proposed the following expression for fatigue life estimation:

$$\frac{\Delta\gamma_{\mathrm{max}}}{2}\left(1 + k\frac{\sigma_{\mathrm{n,max}}}{\sigma_{\mathrm{y}}}\right) = g(N_f) \tag{2}$$

where $\Delta\gamma_{\mathrm{max}}$ remains the same as defined earlier, $\sigma_{\mathrm{n,max}}$ is the maximum normal stress on the plane of maximum shear strain range, σ_{y} is the uniaxial yield strength, k is a material constant, and the right-hand side of Eq. (2) is a function of the number of cycles to failure. The fundamental difference between Eqs. (2) and (1) is the use of the maximum normal stress in the former one, which is introduced as means to account for mean stress and non-proportional hardening effects. The left-hand side of Eq. (2) can be determined by fitting the model to the strain-controlled torsional fatigue curve. Such a procedure yields the following expression:

$$\frac{\Delta\gamma_{\mathrm{max}}}{2}\left(1 + k\frac{\sigma_{\mathrm{n,max}}}{\sigma_{\mathrm{y}}}\right) = \frac{\tau_f'}{G}(2N_f)^{b_0} + \gamma_f'(2N_f)^{c_0} \tag{3}$$

where G is the shear modulus, τ_f' is the shear fatigue strength coefficient, γ_f' is the shear fatigue ductility coefficient, and b_0 and c_0 are shear fatigue strength and shear fatigue ductility exponents, respectively. Different procedures have been used to identify the material constant k. For example, fitting Eq. (3) to the strain-controlled uniaxial fatigue curve yields an expression for k that depends on the fatigue life:

$$k = \left(\frac{\frac{\tau_f'}{G}(2N_f)^{b_0} + \gamma_f'(2N_f)^{c_0}}{\left[(1+\nu_e)\frac{\sigma_f'}{E}(2N_f)^{b} + (1+\nu_p)\varepsilon_f'(2N_f)^{c}\right]} - 1\right)\frac{2\sigma_{\mathrm{y}}}{\sigma_f'(2N_f)^{b}} \tag{4}$$

where ν_e and ν_p are respectively the elastic and plastic Poisson's ratios, E is Young's modulus, σ_f' is the axial fatigue strength coefficient, b is the axial fatigue strength exponent, ε_f' is the axial fatigue ductility coefficient and c is the axial fatigue ductility exponent. As an alternative procedure, the values of k_i that fit Eq. (3) to each uniaxial fatigue test i are first computed. The material constant k is then defined as the arithmetic mean (hereafter denoted as k_{mean}) of the k_i values.

The Brown-Miller and Fatemi-Socie fatigue models are applicable to materials and loading conditions in which crack nucleation and early crack growth are mainly driven by cyclic shear strains. For situations where the fatigue life for crack initiation is controlled by crack growth on planes of maximum normal strain (or stress) amplitude, Socie (1987) proposed a critical plane model based on the Smith, Watson and Topper parameter. Such a fatigue model can be expressed as

$$\frac{\Delta\varepsilon_{\mathrm{n,max}}}{2}\sigma_{\mathrm{n,max}} = \frac{\sigma_f'^2}{E}(2N_f)^{2b} + \sigma_f'\varepsilon'_f(2N_f)^{b+c} \tag{5}$$

where $\Delta\varepsilon_{\mathrm{n,max}}$ is the maximum normal strain range and $\sigma_{\mathrm{n,max}}$ is the maximum normal stress on the plane of maximum normal strain range. The right-hand side of Eq. (5) is obtained by fitting the model to the strain-controlled axial fatigue curve.

2.2 Bannantine-Socie cycle counting method

The method developed by Bannantine and Socie (1991) is a generalization to multiaxial variable amplitude loadings of the well-known uniaxial strain-based approach. Taking as a starting point the fact that fatigue damage has a directional character, the shear strains (or normal strains) acting on each material plane are taken as the main driving forces for crack nucleation. Therefore, rainflow cycle counting is performed on such shear strains (or normal strains).

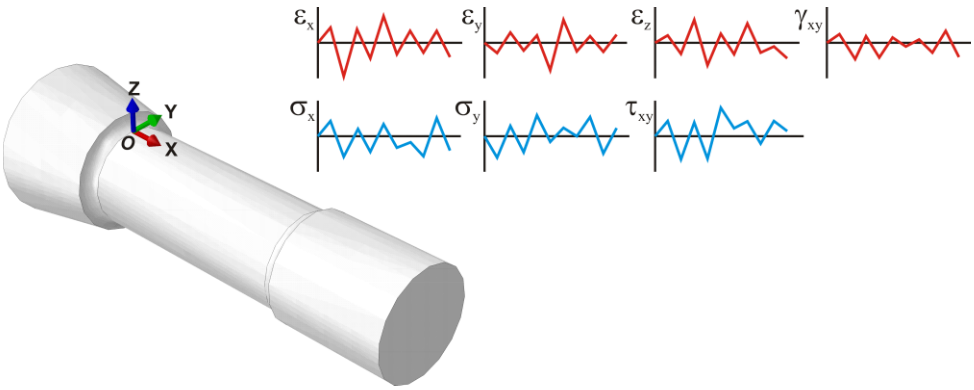

Figure 1. Definition of the *x*-*y*-*z* coordinate system and illustration of corresponding strains and stresses.

Then, a fatigue damage parameter and a damage accumulation rule are used to calculate the damage on each material plane. The critical plane is finally defined as the plane that experiences the maximum fatigue damage.

The Bannantine-Socie method was originally developed for situations where a fatigue crack initiates at a material point *O* located on the free surface of a component (Fig. 1). For a *x*-*y*-*z* coordinate system with the *z*-axis pointing outwards to the surface, the strain and stress tensors ($\boldsymbol{\varepsilon}$ and $\boldsymbol{\sigma}$, respectively) at point *O* have the following forms:

$$\boldsymbol{\varepsilon} = \begin{bmatrix} \varepsilon_x & \frac{1}{2}\gamma_{xy} & 0 \\ \frac{1}{2}\gamma_{xy} & \varepsilon_y & 0 \\ 0 & 0 & \varepsilon_z \end{bmatrix} \qquad \boldsymbol{\sigma} = \begin{bmatrix} \sigma_x & \tau_{xy} & 0 \\ \tau_{xy} & \sigma_y & 0 \\ 0 & 0 & 0 \end{bmatrix} \tag{6}$$

where ε_x, ε_y, … are the strain components and σ_x, σ_y, … are the stress components with respect to the *x*-*y*-*z* coordinate system. To apply the method, the histories of such strains and stresses must be given as input data. Three procedures can be used to achieve this goal: (1) the strains ε_x, ε_y, γ_{xy} are firstly measured with strain gages, and then used to solve a strain-driven elasto-plastic problem whose solution are the stresses σ_x, σ_y, τ_{xy} and the strain ε_z; (2) an elasto-plastic finite element analysis of the component is performed using as input data the applied loadings; and (3) an approximate elasto-plastic analysis is performed using elastic solutions or nominal stress/strain quantities as input data. Once the histories of the strain and stress components have been determined, the following steps are performed:

1) For each material plane defined by angles θ and ϕ (Fig. 2)

   a) Calculate the histories of the shear strains $\gamma_{x'y'}$ and $\gamma_{x'z'}$ and of the normal stress $\sigma_{x'}$ using standard strain and stress transformation rules.
   b) Apply the rainflow cycle counting algorithm to the history of the shear strain $\gamma_{x'y'}$. For each counted cycle i, store the corresponding shear strain range $\Delta\gamma^{(i)}$ and maximum normal stress $\sigma_{\mathrm{n,max}}^{(i)}$.
   c) Compute the fatigue damage caused by each counted cycle i as the fraction of life used up by this cycle:

$$D^{(i)} = \frac{1}{N^{(i)}} \tag{7}$$

   where $N^{(i)}$ is the solution of the Fatemi-Socie equation:

$$\frac{\Delta\gamma^{(i)}}{2}\left(1 + k\frac{\sigma_{\mathrm{n,max}}^{(i)}}{\sigma_{\mathrm{y}}}\right) = \frac{\tau_{f'}}{G}\left(2N^{(i)}\right)^{b_o} + \gamma_{f'}\left(2N^{(i)}\right)^{c_o} \tag{8}$$

   d) Compute the total fatigue damage corresponding to the y'-direction of the plane, $D_{plane,y'}$. Using the Palmgren-Miner damage summation rule, the total damage is defined as the sum of the damages caused by each cycle:

$$D_{plane,y'} = \sum_{i=1}^{n} D^{(i)} \tag{9}$$

where n is the number of counted cycles.

e) Repeat steps b, c and d considering the history of the shear strain $\gamma_{x'z'}$ in order to evaluate total damage corresponding to the z'-direction of the plane, $D_{plane,z'}$.
f) Compute the fatigue damage caused on the material plane, D_{plano}, as the maximum value between the damages corresponding to the y' and z' directions:

$$D_{plano} = \max(D_{plane,y'}, D_{plane,z'}) \tag{10}$$

2) Find the critical plane, i.e. search, amongst all material planes analyzed in step 1, the plane with maximum fatigue damage (D_{max}).
3) Compute the number of repetitions of the loading block until fatigue failure:

$$N_{blocks} = \frac{1}{D_{max}} \tag{11}$$

The procedures described in steps 1b and 1c should be applied only to shear-dominated fatigue cracking mechanisms. For situations involving tensile-dominated mechanisms, the normal strain acting on the material plane should be rainflow counted, and fatigue life should be evaluated with Eq. (5). It should also be mentioned that for a material point located on the free surface of a component, the search for the critical plane does not require an investigation of all planes passing through the point. In the case of a shear-dominated cracking mechanism, only the planes oriented 45° from the z axis (ϕ=45°) and perpendicular to the free surface (ϕ=90°) must be investigated. For a tensile-based cracking mechanism, it suffices to search only the planes perpendicular to the free surface.

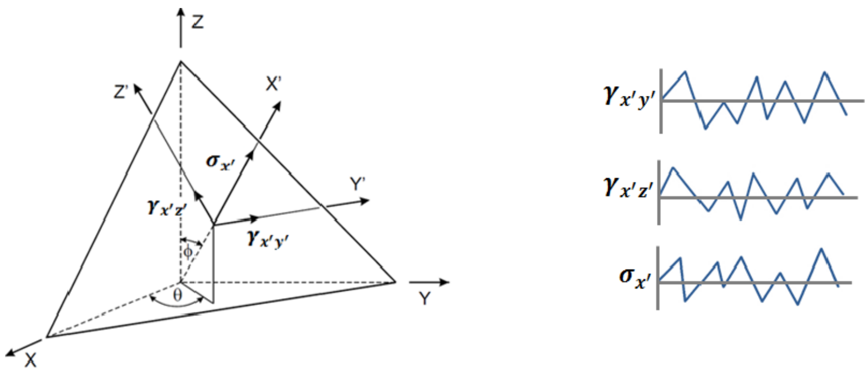

Figure 2. Shear strains and normal stress acting on a material plane defined by angles θ and ϕ.

3. CYCLIC PLASTICITY MODEL

Small strain, rate independent plasticity is adopted in this work. The total strain tensor is additively decomposed into elastic and plastic parts. The elastic strain tensor obeys the isotropic Hooke's law. The plastic strain tensor evolves according to a flow rule associated with the von Mises yield surface

$$F = \sqrt{\tfrac{3}{2}}\|\boldsymbol{S} - \boldsymbol{\alpha}\| - \sigma_0 = 0 \tag{12}$$

where $\boldsymbol{S}$ is the deviatoric stress tensor, $\boldsymbol{\alpha}$ is the deviatoric backstress tensor which defines the center of the yield surface, and σ_0 is the uniaxial yield stress. The backstress tensor was decomposed into additive parts (Chaboche, 1989). More specifically, the following decomposition was adopted:

$$\boldsymbol{\alpha} = \boldsymbol{\alpha}^{(1)} + \boldsymbol{\alpha}^{(2)} + \boldsymbol{\alpha}^{(3)} \tag{13}$$

where the two first parts are governed by Armstrong-Frederick type (nonlinear) evolution laws and the third one obeys a Prager type (linear) evolution law:

$$\dot{\boldsymbol{\alpha}}^{(1)} = \frac{2}{3}c^{(1)}\dot{\boldsymbol{\varepsilon}}^{\boldsymbol{p}} - \zeta^{(1)}\boldsymbol{\alpha}^{(1)}\dot{p} \qquad \dot{\boldsymbol{\alpha}}^{(2)} = \frac{2}{3}c^{(2)}\dot{\boldsymbol{\varepsilon}}^{\boldsymbol{p}} - \zeta^{(2)}\boldsymbol{\alpha}^{(2)}\dot{p} \qquad \dot{\boldsymbol{\alpha}}^{(3)} = \frac{2}{3}c^{(3)}\dot{\boldsymbol{\varepsilon}}^{\boldsymbol{p}} \tag{14}$$

where $c^{(1)}$, $\zeta^{(1)}$, $c^{(2)}$, $\zeta^{(2)}$, $c^{(3)}$ are material constants, $\dot{\boldsymbol{\varepsilon}}^{\boldsymbol{p}}$ is the rate of the plastic strain tensor, and $\dot{p} = \sqrt{2/3}\,||\dot{\boldsymbol{\varepsilon}}^{\boldsymbol{p}}||$ is the accumulated plastic strain rate. It should be noted that no isotropic hardening is used in the current framework.

4. EVALUATION OF THE METHODOLOGY

Strain-controlled axial-torsional fatigue tests available in the literature (Kim and Park, 1999; Kim, Park and Lee, 1999; Kim, Lee and Park, 2000) were used to evaluate the methodology. The materials investigated were a S45C steel and a 304 stainless steel. All specimens had a thin-walled tubular geometry. The different types of constant and variable amplitude loadings were classified as follows:

- For S45C steel: constant amplitude axial tests (A_C), constant amplitude torsional tests (T_C), variable amplitude axial tests (A_VAR), variable amplitude torsional tests (T_VAR), constant amplitude in-phase axial-torsional tests, constant amplitude out-of-phase axial-torsional tests (C_OP), proportional variable amplitude tests (PVAR), alternating axial-torsional tests (AAT), alternating proportional tests (AP), 1 box path test (B), 2 pseudo-random variable amplitude tests (R).
- For 304 stainless steel: constant amplitude axial tests (Axial), constant amplitude torsional tests (Torsion), variable amplitude axial tests (AV), variable amplitude torsion (TV), constant amplitude proportional tests (CP), variable amplitude proportional tests (PV), constant amplitude out-of-phase tests (COP), alternating tension-torsion tests (AAT), alternating proportional tests (AP), box path tests (B), a two-box path tests (TB), pseudo-random loading tests (R), and a butterfly path test (BF).

A detailed description of the experiments can be found in the aforementioned references, including the monotonic and cyclic properties of the materials, the applied strains, and the number of loading blocks until failure.

The constitutive behavior of the material was described by the model presented in Section 3. The procedure to determine the material constans was based on the specialization of the model to uniaxial loading. In this case, it can be shown that the predicted relation between the stabilized values of the stress amplitude, σ_a, and the plastic strain amplitude, ε_{pa}, is

$$\sigma_a = \frac{c^{(1)}}{\zeta^{(1)}}\tanh\zeta^{(1)}\varepsilon_{pa} + \frac{c^{(2)}}{\zeta^{(2)}}\tanh\zeta^{(2)}\varepsilon_{pa} + c^{(3)}\varepsilon_{pa} + \sigma_0. \tag{15}$$

where tanh denotes the hyperbolic tangent function. A power-law curve was used to describe the experimentally obtained values of σ_a and ε_{pa}. The material constants were determined by best fitting of the predicted and experimental curves. Table 1 lists these material constants for the two materials under investigation.

Table 1 – Material constants used in the cyclic plasticiy model.

Material	$c^{(1)}$ (MPa)	$\zeta^{(1)}$	$c^{(2)}$ (MPa)	$\zeta^{(2)}$	$c^{(3)}$ (MPa)	$\zeta^{(3)}$	σ_0 (MPa)
S45C steel	346665	3300	47366	392	12495	0	150
304 steel	343108	3801	38720	424	8368	0	202

After the determination of the material constants, the stress-strain response of the material was simulated using the finite element program Abaqus, version 6.10. The gage section of the tubular specimen was modeled with a single finite element of type PIPE31. The loading and boundary conditions were applied as follows: In one of the nodes, the axial displacement and rotation angle were applied in accordance with the axial and shear strains of each fatigue test. On the other node, all displacements and rotations were prescribed with null values. In each simulation, the loading block was repeated four times in order to achieve the stabilized stress-strain response. Figure 3 illustrates the stabilized stress-strain response of S45C steel when subjected to a pseudo-random axial-torsional strain path.

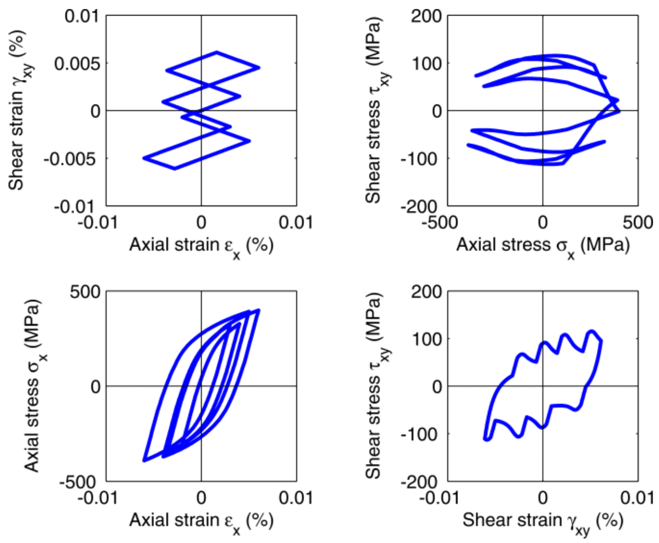

Figure 3. Stress-strain response of S45C steel subjected to a pseudo-random axial-torsional strain path (R01 test).

Figures 4 and 5 show the observed and estimated fatigue lives for the S45C and 304 steels. Fatigue life estimates were computed with the Bannantine-Socie method. Both the Fatemi-Socie and Smith-Watson-Topper parameters were used to evaluate the fatigue damage. In the former case, the two alternative definitions for the material constant k described in Section 2.1 were evaluated, namely the one that expresses $k(N_f)$ as function of the fatigue life and the ther based on the averaged value k_{mean}. In all figures, the central diagonal line represents a perfect agreement between estimated and observed lives, and the other two dashed lines define the factor of two boundaries. Life estimates below the central diagonal line are conservative and the ones above this line are non-conservative.

For the S45C steel, the use of the Fatemi-Socie parameter with $k(N_f)$ yielded life estimates within the factor of two bandwidth for all tests. Considering the well-known scatter of observed fatigue lives, this can be considered a very good correlation. Most life estimates using k_{mean} were within the factor of two bandwidth, the exception being the data point with observed life around 15000 loading blocks and the three data points with observed lives from approximately 100 to 200 loading blocks. The overall correlation produced by the Smith-Watson-Topper parameter was satisfactory, except for some torsional fatigue data (T-C and T-VAR symbols) and for one of the pseudo-random tests (R symbol).

For the 304 steel, fatigue life estimates using the Fatemi-Socie parameter with $k(N_f)$ and k_{mean} were essentially the same. Most of these estimates fell within the factor of two bandwidth, the exception being three fully reversed torsion tests. On the other hand, life estimates based on the Smith-Watson-Topper parameter were not satisfactory for the majority of the constant and variable amplitude torsion tests, one COP test, and one AAT test.

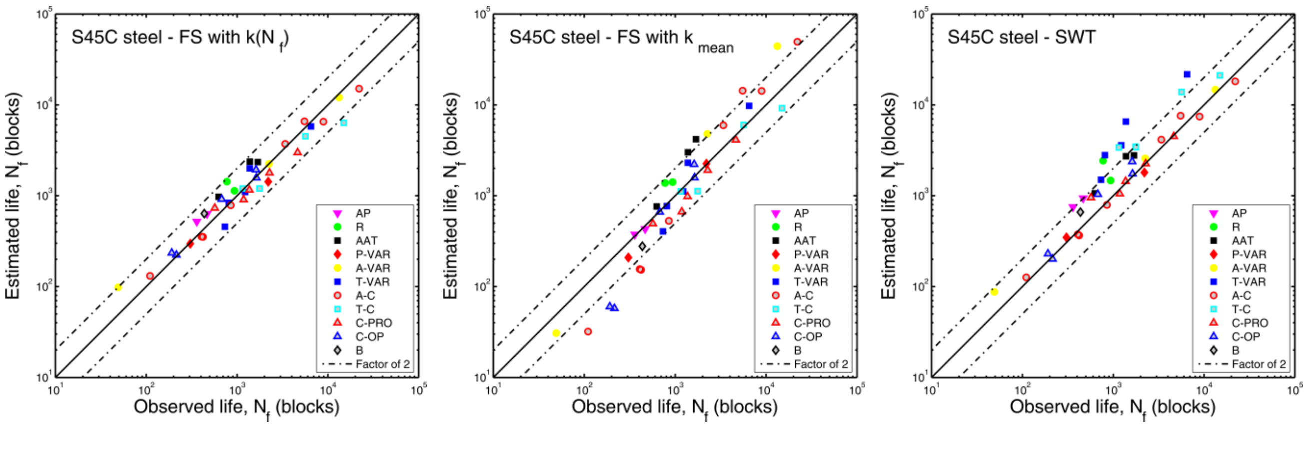

Figure 4. S45C steel - Comparison between observed and estimated lives for the FS parameter with $k(N_f)$ and k_{mean} and for the SWT parameter.

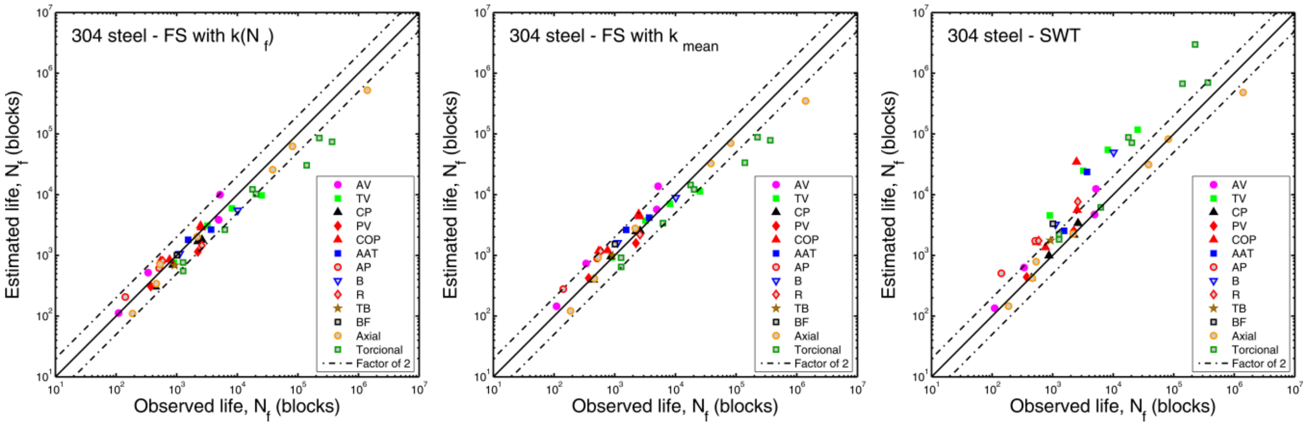

Figure 5. 304 steel - Comparison between observed and estimated lives for the FS parameter with $k(N_f)$ and k_{mean} and for the SWT parameter.

5. CONCLUSIONS

This work presented an evaluation of a fatigue life estimation methodology for general multiaxial loading. In this methodology, Chaboche's kinematic hardening rule is used to calculate the stabilized stress-strain response, and the Bannantine-Socie method is used to estimate crack initiation life. The evaluation was based on available axial, torsional, and combined axial-torsional fatigue tests conducted on tubular specimens of S45C and 304 steels. Constant and variable amplitude loadings were applied to the specimens. Based on the results of the current work, the following conclusions can be drawn:

(1) For the S45C steel, the use of the Fatemi-Socie parameter with $k(N_f)$ yielded life estimates within the factor of two bandwidth for all loading conditions. Similar performance was obtained using k_{mean}, except for four data points. The overall correlation produced by the Smith-Watson-Topper-Socie parameter was satisfactory, except for some torsional fatigue data and for one of the pseudo-random variable amplitude test.
(2) For the 304 steel, fatigue life estimates using the Fatemi-Socie parameter with $k(N_f)$ and k_{mean} were essentially the same. Most of these estimates fell within the factor of two bandwidth, the exception being three fully reversed torsion tests. On the other hand, life estimates based on the Smith-Watson-Topper parameter were not satisfactory for the majority of the constant and variable amplitude torsion tests, one constant amplitude out-of-phase test, and one alternating tension-torsion test.
(3) For both steels, the Fatemi-Socie parameter with $k(N_f)$ yielded the best overall correlation with experimental data. Most fatigue life estimates fell within a factor of two bandwidth, and all estimates outside this band were conservative.
(4) For both steels, fatigue life estimates using the Smith-Watson-Topper parameter were not satisfactory for some of the investigated constant and variable amplitude torsion tests

As a final remark, it should be noted that similar results were obtained in the papers of Kim, Park and Lee listed the References. The difference between their analysis and the present one is that here stresses were simulated using Chaboche's kinematic hardening model, instead of being experimentally determined. As the S45C steel displays a small but not negligible non-proportional hardening effect, while this effect for 304 is pronounced, the use of Chaboche's model to simulate the stress response is not in principle the best available option. However, for the investigated loading paths, the use of less accurate stresses did not resulted in a significant change in the overall life predictions.

6. ACKNOWLEDGEMENTS

The supports provided by CNPq (contracts 310845/2013-0 and 304083/2013-5) are gratefully acknowledged.

7. REFERENCES

Bannantine, J.A. and Socie, D.F., 1991. “A variable amplitude multiaxial fatigue life prediction method”. In: *Kussmaul K, McDiarmid D, Socie D, editors. ESIS10*. London: Mechanical Engineering Publications, p. 35-51.
Brown MW, Miller KJ, 1973. “A theory for fatigue under multiaxial stress–strain conditions”. Proc *Inst Mech Eng*., 187, 745-56.

Chaboche, J.L., 1989. "Time-independent constitutive theories for cyclic plasticity". *International Journal of Plasticity*, Vol. 2, p. 149-188.

Dowling, N.E., 2007. *Mechanical behavior of materials*, Pearson Education, Inc., 3rd edition.

Fatemi, A. and Shamsei, N., 2011. "Multiaxial fatigue: An overview and some approximation models for life estimation". *Int. J. Fatigue*. 33:948-58.

Fatemi, A. and Socie, D.F., 1988. "A critical plane approach to multiaxial fatigue damage including out-of-phase loading". *Fatigue Fract. Eng. Mater. Struct.* 11:149-65.

Kandil FA, Brown MW, Miller KJ, 1982. "Biaxial low-cycle fatigue fracture of 316 stainless steel at elevated temperatures". Book 280. London: The Metals Society, 203-10.

Kim, K.S. and Park, J.C., 1999. "Shear strain based multiaxial fatigue parameters applied to variable amplitude loading". *Int. J. Fatigue*, Vol. 21, p. 475-483.

Kim, K.S., Park, J.C., Lee, B.L., 1999. "Multiaxial fatigue under variable amplitude loads". *J. Eng. Mater. Technol.*, Vol. 121, p. 286-293.

Kim, K.S., Lee, B.L., and Park, J.C., 2000. "Biaxial fatigue of stainless steel 304 under irregular loading". *ASTM STP 1389*, G.R. Halford e J.P. Gallagher, Eds., p. 79-93.

Socie, D.F. and Marquis, G.B., 2000. "Multiaxial fatigue". *SAE International*, Warendale, PA, ISBN 0-7680-0453-5.

Socie, D.F., 1987. "Multiaxial fatigue damage models". *J. Eng. Mater. Technol*. 109, 293-298.

Wang, C. H. and Brown, M. W., 1996. "Life prediction techniques for variable amplitude multiaxial fatigue - Part 1: Theories". *J. Eng. Mater. Technol*., Vol. 118, p. 367-370

Wetzel, R.M., ed., 1977. *Fatigue under complex loading: analysis and experiments*, AE-6, SAE, Warrendale, PA.

8. RESPONSIBILITY NOTICE

The authors are the only responsible for the printed material included in this paper.